Journal of Organometallic Chemistry, 315 (1986) 353–360
Elsevier Sequoia S.A., Lausanne – Printed in The Netherlands

STRUCTURAL, SPECTROSCOPIC AND CONFORMATIONAL STUDIES OF $H_2Ru_2Rh_2(CO)_{11}(PPh_3)$

JOUNI PURSIAINEN and TAPANI A. PAKKANEN

University of Joensuu, Department of Chemistry, P.O. Box 111, SF-80101 Joensuu 10 (Finland)

(Received May 29th, 1986)

Summary

The structure of $H_2Ru_2Rh_2(CO)_{11}(PPh_3)$ has been studied by X-ray crystallography and by NMR spectroscopy. The arrangement of the carbonyl and the hydride ligands is similar to that in $H_2Ru_2Rh_2(CO)_{12}$. The phosphine is equatorially coordinated to the same basal rhodium as the other edge-bridging hydride ligand. A position *cis* to the phosphine is sterically favourable for the bridging hydride.

Introduction

Phosphorus ligands are commonly used in organometallic chemistry and their steric effects have been extensively studied [1]. Relative to mononuclear complexes metal cluster compounds, especially mixed-metal clusters, offer several different sites for phosphine groups and steric restrictions are extended to the ligands on the adjacent metals.

We describe here the structure of $H_2Ru_2Rh_2(CO)_{11}(PPh_3)$ (**1**) in solid state and in solution. The relative steric interactions of the phosphine ligand with the carbonyl and hydride ligands have been studied by computer graphics.

Experimental

The reactions were carried out under N_2 with deoxygenated solvents up to the stage of the chromatographic separations. $H_2Ru_2Rh_2(CO)_{12}$ (**2**), was prepared by a published procedure [2]. Other reagents were obtained from commercial sources and used without purification.

Infrared spectra were recorded on a Perkin–Elmer 297 spectrophotometer using 0.5 mm NaCl solution cells. ^1H and $^{31}P\text{-}\{^1H\}$ NMR spectra were recorded on a Bruker AM-250 spectrometer with $CDCl_3$ as solvent. Chemical shifts are relative to TMS and 85% H_3PO_4, respectively.

0022-328X/86/$03.50

The X-ray fluorescence analysis was carried out with a JEOL 35 CF scanning Electron Microscope equipped with a LINK energy dispersive semiconductor X-ray detector.

Syntheses

$H_2Ru_2Rh_2(CO)_{11}(PPh_3)$. To a solution of 100 mg of **2** in 40 ml of hexane was added a solution of a molar equivalent of PPh_3 in hexane solution. The reaction was rapid at room temperature. The progress of the substitution reaction was followed by IR spectroscopy by use of the peak at 1913 for **2** and that at 2090 cm^{-1} for **1**, since with an excess of PPh_3 the reaction proceeds very readily. After completion of the reaction the mixture was chromatographed immediately on silica gel (15 cm column). Hexane eluted some yellow $H_4Ru_4(CO)_{12}$ and also orange unchanged **2**. A 10/1 hexane/CH_2Cl_2 mixture then eluted a yellow fraction and finally a red fraction of **1** (72 mg, 55%). $\nu_{max}(CO)$ 2090m, 2065vs, 2056m, 2044vs, 2030s, 2023sh, 2008w, 1998w, 1880w, 1860m. Semiquantitative elemental determinations of ruthenium and rhodium were made by X-ray fluorescence. The shape of the Ru/Rh peak was similar to that of the parent cluster [3], indicating a 2/2 metal ratio.

X-ray crystallography

Crystals of **1**, suitable for X-ray analysis were obtained by recrystallisation from hexane/dichloromethane. Unit cell parameters were determined by least-squares refinement for 14 automatically centered reflections in the range $22 < 2\theta < 24°$. The crystal data and details of the data collection are summarised in Table 1. Intensity

TABLE 1

CRYSTAL DATA AND DETAILS OF STRUCTURE ANALYSIS OF $H_2Ru_2Rh_2(CO)_{11}(PPh_3)$

Crystal data	
Formula	$Ru_2Rh_2C_{29}O_{11}H_{17}P$
M	980.0
Crystal system	Monoclinic
a (Å)	10.220(2)
b (Å)	14.571(3)
c (Å)	22.354(4)
β (°)	102.45(1)
V ($Å^3$)	3251(1)
Space group	$P2_1/c$
Z	4
D_c ($g\ cm^{-3}$)	2.00
$F(000)$	1887.8
Linear absorption coefficient (Mo-K_α)	19.6 cm^{-1}
Data collection using Mo-K_α radiation (λ 0.71069 Å)	
$\theta_{min}, \theta_{max}$	2.5–25°
Total data	6461
Observed data $I > 2.5\sigma(I)$	4655
Merging R factor	0.0471
Refinement	
No. of parameters	406
Final R	0.0404
R_w ($w = 1/[\sigma^2(F) + 0.005F_2]$	0.0410

TABLE 2

ATOMIC COORDINATES AND TEMPERATURE FACTORS (Å^2 ×10^3) FOR **2**

Atom	*x*	*y*	*z*	*U* [a]
Ru(1)	0.35353(5)	0.17614(3)	0.20999(2)	37.7(2)
Ru(2)	0.35635(5)	0.34892(3)	0.14415(2)	41.2(2)
Rh(1)	0.12923(5)	0.23747(3)	0.12944(2)	43.9(2)
Rh(2)	0.20523(4)	0.33781(3)	0.23219(2)	34.3(1)
P(1)	0.1930(1)	0.3569(1)	0.33482(6)	34.2(4)
O(2)	0.0353(6)	0.4980(4)	0.1804(3)	78(2)
O(3)	0.6239(7)	0.3803(5)	0.1107(4)	106(3)
O(4)	0.2382(7)	0.5192(4)	0.0753(3)	100(3)
O(5)	0.0422(7)	0.0536(4)	0.0715(3)	98(3)
O(6)	−0.0976(8)	0.3500(6)	0.0516(3)	122(4)
O(7)	0.2166(7)	0.0309(4)	0.2718(3)	90(3)
O(8)	0.3956(5)	0.0408(3)	0.1122(2)	61(2)
O(9)	0.6217(6)	0.1408(4)	0.2987(3)	88(3)
O(10)	−0.174(5)	0.1929(4)	0.2316(2)	74(2)
O(11)	0.4690(5)	0.4467(3)	0.2666(2)	57(2)
O(12)	0.2923(6)	0.2291(4)	0.0288(2)	75(2)
C(2)	0.0966(7)	0.4373(5)	0.2012(3)	51(2)
C(3)	0.5223(8)	0.3715(5)	0.1231(4)	62(3)
C(4)	0.2810(8)	0.4552(5)	0.1009(3)	62(3)
C(5)	0.0762(7)	0.1204(5)	0.0944(3)	58(3)
C(6)	−0.0125(8)	0.3082(6)	0.0800(4)	72(3)
C(7)	0.2653(7)	0.0863(4)	0.2475(3)	55(2)
C(8)	0.3832(6)	0.0913(4)	0.1481(3)	47(2)
C(9)	0.5225(8)	0.1547(5)	0.2664(3)	56(3)
C(10)	0.0556(7)	0.2326(5)	0.2079(3)	51(2)
C(11)	0.3958(6)	0.4070(4)	0.2297(3)	40(2)
C(12)	0.2801(8)	0.2612(5)	0.0736(3)	55(2)
C(20)	0.2869(6)	0.2658(4)	0.3816(3)	40(2)
C(21)	0.4233(6)	0.2737(5)	0.4025(3)	49(2)
C(22)	0.4974(8)	0.1997(5)	0.4319(3)	64(3)
C(23)	0.4337(9)	0.1198(5)	0.4392(3)	71(3)
C(24)	0.3022(9)	0.1102(5)	0.4168(4)	70(3)
C(25)	0.2251(8)	0.1825(4)	0.3881(3)	52(2)
C(30)	0.2561(6)	0.4643(4)	0.3727(3)	38(2)
C(31)	0.2998(7)	0.4705(4)	0.4365(3)	48(2)
C(32)	0.3371(7)	0.5536(5)	0.4637(3)	58(3)
C(33)	0.3289(7)	0.6319(5)	0.4296(3)	61(3)
C(34)	0.2842(7)	0.6271(4)	0.3670(3)	53(2)
C(35)	0.2484(6)	0.5438(4)	0.3384(3)	46(2)
C(40)	0.0259(6)	0.3483(4)	0.3518(3)	43(2)
C(41)	−0.0872(6)	0.3610(5)	0.3065(4)	55(2)
C(42)	−0.2124(7)	0.3567(5)	0.3193(4)	71(3)
C(43)	−0.2249(8)	0.3418(6)	0.3778(5)	78(4)
C(44)	−0.1135(8)	0.3305(6)	0.4241(4)	75(3)
C(45)	0.0104(7)	0.3336(5)	0.4114(3)	58(3)
H(1)	0.450	0.256	0.179	
H(2)	0.317	0.253	0.266	

[a] Equivalent isotropic *U* defined as one third of the trace of the orthogonalized *U* tensor.

TABLE 3

SELECTED BOND LENGTHS (Å)

Ru(1)–Ru(2)	2.920(1)	Ru(1)–Rh(1)	2.742(1)
Ru(1)–Rh(2)	2.901(1)	Ru(2)–Rh(1)	2.794(1)
Ru(2)–Rh(2)	2.756(1)	Rh(1)–Rh(2)	2.692(1)
Ru(1)–C(7)	1.886(7)	Ru(1)–C(8)	1.927(7)
Ru(1)–C(9)	1.932(7)	Ru(2)–C(3)	1.885(9)
Ru(2)–C(4)	1.899(7)	Ru(2)–C(11)	2.051(6)
Ru(2)–C(12)	2.049(6)	Rh(1)–C(5)	1.907(7)
Rh(1)–C(6)	1.922(8)	Rh(1)–C(10)	2.053(7)
Rh(1)–C(12)	2.209(8)	Rh(2)–P(1)	2.341(2)
Rh(2)–C(2)	1.867(7)	Rh(2)–C(10)	2.151(7)
Rh(2)–C(11)	2.204(6)	O(2)–C(2)	1.125(9)
O(3)–C(3)	1.137(11)	O(4)–C(4)	1.131(9)
O(5)–C(5)	1.118(9)	O(6)–C(6)	1.137(11)
O(7)–C(7)	1.145(10)	O(8)–C(8)	1.117(8)
O(9)–C(9)	1.129(9)	O(10)–C(10)	1.159(9)
O(11)–C(11)	1.144(7)	O(12)–C(12)	1.136(9)

data were collected on Nicolet R3m diffractometer using graphite monochromated Mo-K_α radiation. The data were corrected for Lorenz and polarisation effects and absorption.

The structure was solved by the direct methods of the SHELXTL program package [4] and Fourier synthesis. Non-hydrogen atoms were refined anisotropically and organic hydrogen atoms were placed in calculated positions (C–H 0.96 Å). Hydride ligands were judged to be located at the edge-bridging positions on the basis of the steric effects on the nearest ligands and of the lengthening of the relevant metal–metal bonds. Hydrogen positions were also indicated but could not be refined. The metal atoms were not identified crystallographically, but they were refined as two Ru and two Rh atoms in positions consistent with the NMR data. These positions were also suggested by difference Fourier maps of the otherwise fully refined structure, and changes could be seen when the metal arrangement was changed. The quality of the data, however, was not good enough for reliable direct metal assignment. The final R and R_w were 0.0404 and 0.0410.

TABLE 4

SELECTED BOND ANGLES (°)

Ru(2)–Ru(1)–C(8)	99.9(2)	Ru(2)–Ru(1)–C(9)	111.4(2)
Rh(1)–Ru(1)–C(7)	96.1(2)	Rh(1)–Ru(1)–C(8)	88.6(2)
Rh(2)–Ru(1)–C(7)	99.8(2)	Rh(2)–Ru(1)–C(9)	116.5(2)
Ru(1)–Ru(2)–C(3)	112.6(2)	Rh(1)–Ru(2)–C(4)	100.3(2)
Rh(2)–Ru(2)–C(4)	100.6(3)	Ru(1)–Rh(1)–C(5)	95.8(2)
Ru(2)–Rh(1)–C(6)	105.1(3)	Rh(2)–Rh(1)–C(6)	104.1(2)
Ru(1)–Rh(2)–P(1)	113.9(0)	Ru(2)–Rh(2)–C(2)	94.0(2)
Rh(1)–Rh(2)–C(2)	93.8(2)	Rh(1)–C(10)–O(10)	143.0(5)
Rh(2)–C(10)–O(10)	137.1(5)	Ru(2)–C(11)–O(11)	147.9(6)
Rh(2)–C(11)–O(11)	131.2(5)	Ru(2)–C(12)–O(12)	147.0(7)
Rh(1)–C(12)–O(12)	131.1(6)		

The fractional coordinates are given in Table 2, selected bond lengths in Table 3, and selected bond angles in Table 4.

Conformational studies

The Chem-X computer graphics system [5] was used for the calculations. The Van der Waals interaction energy was calculated for the structure changes using the following expression for the energy:

$$\{A \cdot \exp(-Br)/r^D\} - (C/r^6) + (kq_1q_2/r)$$

where A, B, C and D are constants
q_1 and q_2 are atomic charges
k is a unit conversion factor
r is the distance between the atom pair

The interaction parameters for C, H and O atoms were given in the program. Interactions involving phosphorus and metal atoms were not included.

Results and discussion

X-Ray crystallography

The molecular structure of **1** is shown in Fig. 1. The arrangement of the ligands is fully consistent with the parent cluster. The edge-bridging positions for the hydrides were deduced from the long metal–metal bonds and the opening of the nearest metal–metal–ligand bond angles (see Tables 3 and 4), which are closely related to the values in the crystal structure of **2**. In particular, the Ru(1)–Ru(2)–C(3) (112.6°) and Ru(1)–Rh(2)–P(1) (113.9°) angles differ distinctly form the Ru(1)–Rh(1)–C(5) (95.8°) angle.

The bridging carbonyls are not symmetrical. CO(11) and CO(12) have stronger bonds to Ru(2) than to the rhodium atoms, as indicated by the fact that the Ru(2)–C bonds are about 0.15 Å shorter and the Ru(2)–C–O bond angles about 16° larger (Tables 3 and 4). Otherwise Ru(2) would be electron deficient. In addition, CO(10) coordinates more strongly to Rh(1) than to Rh(2), which would be electron-rich due to the hydride ligand. This, however, contrasts with the crystal structures of $Rh_4(CO)_{10}(PPh_3)_2$ [6] and $Co_4(CO)_{11}(PPh_3)$ [7], where the shorter M–C bonds and larger M–C–O angles are associated with the phosphine-bonded metal atoms. In the crystal structure of **2**, where there was evidence of mutual disorder between Ru(2) and Rh(2), there is no clear evidence of asymmetry of the bridging carbonyls. The crystal structure of $Rh_4(CO)_{12}$ contains indications of one asymmetrical carbonyl bridge but the standard deviations were substantial [8].

The phosphine is coordinated equatorially, which is also the case in $Rh_4(CO)_{11}(PPh_3)$ [6]. In $Co_4(CO)_{11}(PPh_3)$ [7] an axial site is occupied. Opening of the bond angle observed for Ru(1)–Ru(2)–C(3) and Ru(1)–Rh(2)–P(1) is also found in $Rh_4(CO)_{10}(PPh_3)_2$ (Rh_{ap}–Rh_{bas}–P_{eq} 108°) due to steric constraints imposed by the bulky phosphine ligand. The corresponding average value for $Rh_4(CO)_{12}$ is only 95° [8]. Therefore, in **1**, the equatorial position *cis* to a hydride ligand is sterically favourable for the phosphine, since both the phosphine and the hydride cause similar distortions for structures independent of each other. This effect has been previously observed in tetranuclear Os_3Pt cluster compounds [9].

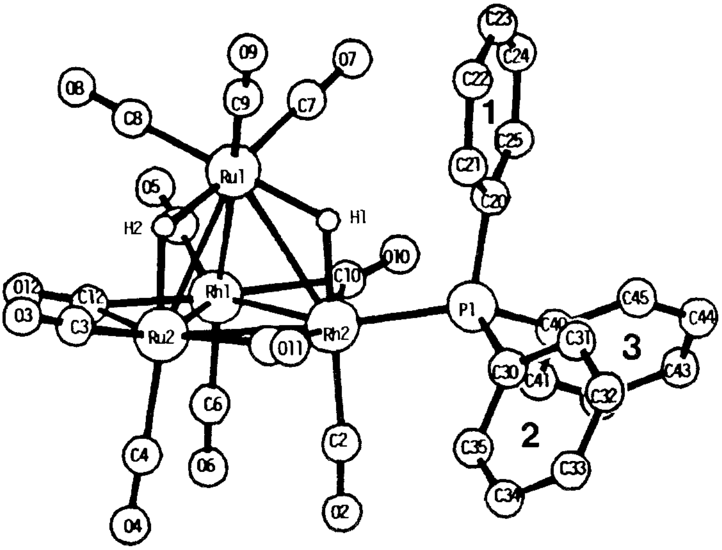

Fig. 1. The crystal structure of $H_2Ru_2Rh_2(CO)_{11}(PPh_3)$.

Conformational studies

Theoretically the hydrogen atoms on C(21) or on C(25) could be at a distance of 1.2 Å from H(1), which would cause strong steric repulsions. In Fig. 2 a Van der Waals repulsion energy map is shown for the rotation of Ph(1) (Fig. 1) around the P(1)–C(20) bond. Ph(2) and Ph(3) were omitted in order to restrict the study to the

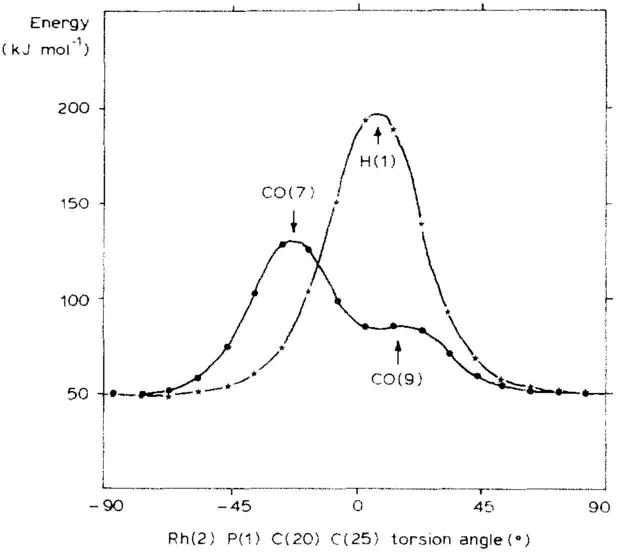

Fig. 2. The Van der Waals repulsion energy (kJ mol^{-1}) for the rotation of Ph(1) without CO(7) and CO(9) (●) and without H(1) (★) in the model. Ph(2) and Ph(3) were omitted.

environment of H(1). The nearest apical carbonyls and H(1) were omitted one at a time in order to see their steric effects on Ph (1). The rotation of Ph(1) is limited by CO(7) in the negative range of Rh(2)–P(1)–C(20)–C(25) torsion angles and simultaneously by CO(9) and H(1) with positive angles. The orientation of lowest energy (Rh(2)–P(1)–C(20)–C(25) torsion angle $-86.4°$) was independent of the presence of H(1). When Ph(2) and Ph(3) and the apical carbonyls were present the absence of H(1) caused differences in the repulsion energy only at a level of 130 kJ mol^{-1} above the lowest energy.

These results indicate qualitatively that the orientation of Ph(1) is determined by the carbonyls and by the other phenyl groups. Such orientations, in which the mutual steric constraints of the phosphine and H(1) could be significant, are also forbidden by the other ligands. It can be said that a sterically favourable 'hole' is created for a hydride *cis* to the phosphine substituent. Any other position for H(1) would increase the steric pressure on the phosphine as a result of bond angle opening elsewhere in the molecule.

NMR spectroscopy

The ^{1}H NMR spectrum of **2** at $-40°$C is consistent with the crystal structure. The chemical shifts of the hydride ligands differ only slightly from the parent cluster and the coupling pattern indicates that a Ru–Ru and a Ru–Rh edge are occupied. The signal from H(1) (-19.7 ppm., ^1J(Rh(2)–H(1)) 17.7, ^2J(P(1)–H(1)) 9.4, ^3J(H(2)–H(1)) 2 Hz) is fully consistent with the crystal stucture. The Ru(μ-H)Ru position for H(2) is evidenced by a signal for which no large couplings can be detected (-21.0 ppm). On decoupling at the H(1) frequency the coupling to P(1) can be seen (^3J(P(1)–H(2)) 1.6 Hz). A similar ^3J(P–H) value was previously observed, e.g., in the phosphine derivatives of $H_2FeRu_3(CO)_{13}$ [9]. No ^2J(Rh–H) couplings were observed in the parent cluster, and on decoupling at the H(2) frequency only the couplings to Rh(2) and P(1) were seen for the H(1) signal. The phosphine substitution induces slightly more electronic shielding for H(1) (-19.2 ppm in **2**) and deshielding for H(2) (-21.3 ppm in **2**). At -20 and at $+2°$C no changes were observed in the peak width of the H(2) resonance, whereas the H(1) signal coalesced into a broad signal with no couplings detectable. The 1/1 intensity ratio and chemical shifts did not change. At room temperature the H(2) peak also broadened. In the absence of the coupling information we can only speculate that the broadenings show the onset of Rh(1)HRu – Rh(2)HRu and RhHRu – RuHRu exchange processes, such as were observed in **2**.

The ^{31}P-{^{1}H} NMR spectrum of **1** consists of a doublet between -40 and $+23°$C (at 38.4 ppm, ^1J(Rh(1)–P(1)) 130 Hz), showing that the phosphine is coordinated to rhodium. The smaller couplings were hidden because of the breadth of the signal (the peak width was 21 Hz at $-40°$C and about 65 Hz at $+10°$C).

Acknowledgements

We thank Dr. J. Jääskeläinen for the X-ray fluorescence analysis.

References

1 C.A. Tolman, Chem. Rev., 77 (1977) 313.
2 J. Pursiainen, T.A. Pakkanen, B.T. Heaton, C. Seregni and R.G. Goodfellow, J. Chem. Soc., Dalton Trans., (1986) 681.

3 J. Pursiainen, T.A. Pakkanen and J. Jääskeläinen, J. Organomet. Chem., 290 (1985) 85.

4 G.M. Sheldrick, The SHELXTL System, Revision 2.5, Nicolet Co., Madison, Wisconsin, 1980.

5 Chem-X, created by E.K. Davies, Chemical crystallography Laboratory, Oxford university, Oxford, 1986.

6 B.T. Heaton, L. Longhetti, D.M.D. Mingos, C.E. Garlaschelli and U. Sartorelli, J. Organomet. Chem., 213 (1981) 333.

7 D.J. Darensbourg and M.J. Incorvia, Inorg. Chem., 20 (1981) 1911.

8 C.H. Wei, Inorg. Chem., 8 (1964) 2384.

9 L.J. Farrugia, M. Green, D.R. Hankey, M. Murray, A.G. Orpen and F.G.A. Stone, J. Chem. Soc., Dalton Trans., (1985) 177.

10 W.L. Gladfelter, J.R. Fox, J.A. Smegal, T.G. Wood and G.L. Geoffroy, Inorg. Chem., 20 (1981) 3223.